Accepted Manuscript

Experimental mechanical characterization of composite-concrete joints

J. Justo, F. París

PII: S1359-8368(18)30261-0
DOI: 10.1016/j.compositesb.2018.08.002
Reference: JCOMB 5832

To appear in: *Composites Part B*

Received Date: 20 February 2018
Revised Date: 24 July 2018
Accepted Date: 2 August 2018

Experimental mechanical characterization of composite-concrete joints

J. Justo, F. París

Grupo de Elasticidad y Resistencia de Materiales, E.T.S. Ingeniería, Universidad de Sevilla, España.

Abstract

The use of composite materials as a reinforcement for concrete in civil construction has become a significant topic, the quality of the joint between composite and concrete being one of the key parameters to study. The preparation of surfaces involved in the joint and the fabrication procedure are relevant factors in this quality. Two surface treatments of concrete (grinder and grit sandpaper) and three manufacturing techniques of the composite and corresponding joining to the concrete (precured composite, wet hand lay-up and infusion) have been employed. To evaluate the quality of the joint, four tests have been applied: Lap peeling, Lap shear, Pull off and Shear torsion. Once the tests were carried out, all of them were found representative of the quality of the joint and it was observed that concrete cracking predominates over adhesive or cohesive failures, which indicates a satisfactory adhesion between the concrete and the composite. Grinder surface treatment was found the best option, and with reference to the manufacturing technique, the use of pre-fabricated reinforcement was found to lead to undervalues of the properties.

Keywords: composite material; concrete; joining; testing; surface treatment

1. Introduction

There is currently a large effort in investigating new strengthening systems for concrete structures based on composite materials, developing current knowledge and generating new related technologies that are sustainable and respectful of the environment. Rehabilitation through structural strengthening is where composite materials has found a large field of application both for masonry and concrete structures. First, the rehabilitation or strengthening of structures is executed to increase their useful life. Rehabilitation can be carried out in structures that are damaged, poorly executed or that simply require a greater carrying capacity as a result of increased demands. Second, composite materials do not present degradation by corrosion and are very resistant to chemical attack, so their use in strengthening would allow solutions to be obtained with practically no need for maintenance and, by extension, with greater durability and sustainability than those of traditional repairs [1, 2], especially if their fire resistance is improved. Because these strengthening systems are still under development, the associated tests are also at an early stage. In this way, many of the tests found in the literature are proposed by different researchers and are not standardized. Despite this, many international research institutions have proposed several design guidelines and test protocols, like those of the Fédération internationale du béton [3] or the Italian National Research Council [4].

An appropriate strengthening of the structures is required to achieve the highest possible properties of the joint of the concrete with the composite material. These properties of the joint are conditioned by several factors:

1. Related to the concrete substrate: the surface treatment and the strength of the concrete itself [5, 6, 7, 8].

2. Related to the composite: the type of resin and fibres, the stacking sequence, the manufacturing technique [9] and the curing temperature [10].

3. Related to the adhesive: the type of adhesive chosen and the manufacturing technique of the joint [11, 12].

4. Related to the environment: the temperature, moisture and frost/thaw cycle during the manufacturing of the joint and during its service life [13].

The possible failures of the concrete-composite joint, motivated by the factors previously described, are summarized in Figure 1:

a) and g) Describe the failure of the concrete;

b) Describes the failure of the composite, with a breaking of the fibres;

c) Describes the failure of the adhesive, also known as cohesive failure;

d) Describes the delamination of the plies of the composite;

e) Describes the failure of the concrete-adhesive interface (a kind of adhesive failure);

f) Describes the failure of the composite-adhesive interface (another kind of adhesive failure).

When the composite-concrete joint is correctly realised, the failure must be associated with the cracking of concrete. When this type of failure occurs, cracks begin to appear in the concrete at a depth of several millimetres below the concrete-adhesive interface. These cracks propagate and lead the specimen to failure. It can therefore be said that the strength of concrete is a relevant parameter controlling the response of FRP-to-concrete joint.

In this work, the quality of the concrete-composite joint will be evaluated under several conditions. Two different surface treatments for concrete, grinder and grit sandpaper, will be used in order to check how the aggressiveness of the treatment conditions the results. Three different manufacturing techniques for the composite and the joint (pre-manufacturing, in situ wet hand lay-up and infusion) have been conceived and applied where the test allows their use. Finally, four different tests will be used to evaluate the quality of the joint under different stress states (note that two of the tests, Pull off and Lap shear, have been adopted by the Italian National Research Council in their guidelines [4])

In section 2 of this work, the tests used to characterize the quality of the joint and the coupons needed to carry out the tests are described. In the tests, the forces needed to debond the composite of the concrete will be characterized, i.e., pull off, peeling and shear forces. The results and discussion are presented in section 3. Finally, the conclusions of the work are summarized in section 4.

2. Joint characterization tests and coupons description

2.1 Characterization tests

2.1.1 Lap peeling test

In this test, a peeling force is applied to the joint [14]. A composite laminate is partially bonded to a concrete block, leaving some zone of the laminate free to move (see Figure 2(a)). The force is applied at the free edge of the composite laminate, following the direction perpendicular to the bonding plane (along the y-direction). The concrete block rests over rolls in order to allow it to move perpendicular to the load (along the x-direction) and to avoid the appearance of traction effects other than those directly derived from the peeling force. The movement of the concrete along the y-direction is restrained by the own weight of the block. The test ends when all the laminate has been peeled off from the concrete.

The Lap peeling tests have been performed in an Instron 4482 electromechanical testing machine. To release the movement perpendicular to the load of the concrete block, it is placed over a tool that is in turn placed over the rolls (the concrete block was not placed directly over the rolls because of the irregularities of the concrete, which could have blocked the rolls), as seen in Figure 3(a). For clamping the composite laminate to the testing machine, a specific tool has been designed and manufactured (Figure 3(b)). It allows the gripping zone to rotate when the load is applied, as the peeling of the composite tends to do, thus avoiding the introduction of undesired stresses due to the fixation of the coupon.

2.1.2 Lap shear test

In this test, a shear force is applied to the joint. The coupon configuration is the same as described for the lap peeling test. In this case, the concrete block is fixed, inhibiting all of its movements. The load is applied at the free edge of the composite laminate, following the x-axis, as shown in Figure 2(b). The test ends when the laminate is separated from the concrete block. These tests have also been carried out in an Instron 4482 testing machine. The laminate has been loaded with the upper grip of the machine (Figure 4). The concrete block has been fixed to the machine using a steel fixture designed for this purpose.

2.1.3 Pull off test

In this test, a pulling load is applied perpendicular to the joint [15, 16]. In this case, a composite laminate is fully bonded to a concrete block. Then, both elements are trepanned until reaching a certain depth in the concrete block, obtaining circular coupons (see Figure 5(a)). To allow the force to be applied to the composite laminate, a metallic block is bonded to it, by using an adhesive with better mechanical properties than those of the composite-concrete joint that is the object of the study. The load is applied to the metallic block and is perpendicular to the bonding plane. The movements of the concrete block are fully constrained. The test ends when one of the adherents is pulled off.

This test has been carried out following the standard ASTM D4541 [17]. The tests have been performed using a standard Proeti pull off strength tester machine (Figure 6(a)), traditionally used in the test to measure the quality of tile bonding to the concrete, as those proposed by Czaderski et al [18]. The equipment is manual, and it is actuated through a crank. The equipment has a load cell that measures the force applied. It has three adjustable legs that regulate the position of the equipment over the coupon to be tested. To connect the machine to the coupons and apply tension, a bolt that is gripped by the machine is screwed into the metallic block that is bonded to the top of the coupons (Figure 6(b)).

The equipment only determines the maximum load that the coupon is able to withstand, so the load-displacement evolution along the entire test was not recorded.

2.1.4 Shear torsion test

In this test, a torsional shear load is applied to the joint. The coupons are the same as those described for the pull off test. In this case, the applied load is a torque, and it is directly applied to the metallic block

(Figure 5(b)). The test ends when one of the adherents is debonded. To carry out this test, a torque wrench has been used. The wrench is actuated over a crank that is screwed to the load cylinders bonded to the composite material. In this way, a torque is transmitted to the composite-concrete joint. The torque wrench used is discrete and only allows a maximum torque to be fixed but does not measure the actual torque applied. In this way, the torque was applied in steps of 5 Nm. The failure torque was obtained as the mean of the values between the ultimate and the penultimate maximum torque fixed in the wrench when the failure of the coupon occurred. To avoid possible movements of the concrete block, it was fixed with clamps. A view of the loading fixture is shown in Figure 7.

2.2 Coupons definition and manufacturing

The geometries and the manufacturing of the coupons for each kind of test are described next. For each configuration, 5 coupons have been tested. Combining the different types of tests, manufacturing methods for the composite (1 for the lap shear and lap peeling tests and 3 for the other tests) and surface treatments for the concrete, a total of 80 coupons have been tested.

The concrete used has a characteristic strength of 35 MPa. The composite, in all cases, is formed by 3 layers of carbon fibre/epoxy UD tape material, with all layers oriented in the same direction and the fibres placed coinciding with the longitudinal direction of the coupon. The number of layers was selected based on regular practice in repairing/strengthening of concrete structures. The carbon fibres have a tensile strength of 4900 MPa and a tensile modulus of 230 GPa and the resin a tensile strength of 85 MPa and a tensile modulus of 3.5 GPa

2.2.1 Lap peeling and lap shear coupons

As mentioned before, the geometry of the coupons in these tests is the same. The geometric characteristics of both the concrete block and the composite laminate are described in Figure 8. The bonding length has been fixed to 200 mm, enough to appropriately transmit the load between the adherents. This length has been chosen based on previous studies [19], which describe a minimum effective bonding length between 90 mm and 160 mm.

To avoid unexpected cracks at the border of the concrete block, due to the presence of the corner (these failures were observed in the preparation stages of this work), an unbonded zone (with the length L_{free} referred to in Figure 8) has been disposed, as suggested in [15].

The manufacturing of the coupons is described as follows:

- The composite laminate was manufactured by the hand wet lay-up method, in which the resin is added manually to dry fibre preforms. The coupon was allowed to cure completely in a convection oven at 60°C for 24 hours.
- The block is sanded in order to prepare it for bonding. Two surface treatments were applied to different faces of the blocks: grinder and grit sandpaper. In this way, the same block was used for bonding several composite laminates, discarding the face of the block that was in contact with the air during the consolidation of the concrete (it usually contains defects and, in this way, lower mechanical properties than the other faces).
- The concrete block is protected with a demoulding layer (Figure 9(a)), leaving a free zone where the laminate will be bonded. In this way, an undesired flow of the adhesive is avoided.
- Once the laminate is cured, it is bonded to the concrete block (Figure 9(b)) using the same resin of the composite material, allowing it to cure at 60°C for 24 hours under a pressure of 0.28 MPa. From this point on, this method will be called precured composite bonding.

2.2.2 Pull off and shear torsion coupons

The geometry of the coupons for both tests is the same. As mentioned before, the coupons consist of a composite laminate bonded to a concrete block, with a metallic block joined to it in order to apply the load. A scheme for the coupons and their dimensions is shown in Figure 10.

The composite was manufactured using three different techniques: bonding of precured laminate [18], in situ hand lay-up [20] and infusion [21]. The procedures are described next.

Bonding of precured laminate: the procedure is the same as described in section 2.2.1.

In situ hand lay-up: in this case, a wet hand lay-up of the composite is made over the concrete, using the resin of the laminate as an adhesive between the composite and the concrete. The curing process is the same as described before.

Infusion: in this case, the dry fibre is placed over the concrete block. Then, a vacuum bag is made to envelop them. A resin tank is connected to the vacuum bag, and the vacuum is performed inside the bag using a pump. Due to the air removal, the resin is sucked from the tank and spread inside the bag, wetting the fibres and the concrete and bonding them. The set is cured as described in 2.2.1.

Once the set is bonded, a trepanation must be performed. To this end, a drilling machine with a tungsten carbide circular crown was used (see Figure 11(a)). It is important to mention that during the trepanation, cooling the material with water is absolutely needed due to the high temperature reached when the concrete is trepanned (the absence of cooling leads to a burning of the resin).

Finally, the metallic block is bonded to the composite inside the trepanation using an EA-9394 high-strength bi-component adhesive (in order to avoid the failure of this joint).

To minimise the number of concrete blocks used, several coupons have been extracted from each block (Figure 11(b)), leaving a separation between the coupons of at least 2 cm, which avoids interference between the coupons.

3. Tests results and discussion

3.1 Lap peeling tests

The results obtained for the five coupons with both grinder and grit sandpaper surface treatments are presented in Figures 12 and 13, respectively (the displacements have been measured with the crosshead of the testing machine and represent the vertical component of the movement of the composite laminate). In both cases, a linear evolution is obtained until reaching the maximum load. After this, debonding appears to grow throughout the interphase, which is accompanied by a decrease in the load. In the case of the grinder-treated coupons, the load increases after each decreasing peak, whereas in the grit sandpaper-treated coupons, this effect is not as obvious, and the load decreases fast and remains almost constant.

The mean of the values obtained for each set of coupons, the standard deviation and the covariance are shown, for both cases, in Table 1. It has also been included, for this table and the following ones, the percentage of the maximum mean load (in parentheses, at the right of the mean maximum loads) taking as reference the minimum mean value, in order to facilitate the comparison between surface treatments and manufacturing methods. It can be seen that for the case of the grinder-treated coupons, the peak loads obtained are higher, and the dispersion of the values is smaller than for the case of the grit sandpaper-treated coupons.

The differences in the load-displacement curves and in the results obtained for both surface treatments can be explained by observing the failure surfaces of the coupons after the tests (Figures 14(a) and 14(b)). In the grit sandpaper-treated coupons, the cracks have propagated throughout the adhesive and the concrete at a superficial level (a mix of concrete and resin existing in this zone), producing a cohesive failure. In the case of the grinder-treated coupons, the surface presents different zones, causing concrete failure at a deep level (including the breaking of stones) and showing also both cohesive and adhesive failures (Figure 15). The level of adhesion is higher in the case of the grinder-treated coupons, giving higher load values. The adhesive and cohesive failures can be explained by the irregularities of the surface of the concrete block that do not let the composite laminate to be correctly bonded at certain zones. The presence of the different zones explains the changing load-displacement evolution seen in Figure 12 after the maximum load, where the load increases after periods of decreasing. It is noticeable that despite the intrinsic inhomogeneity of concrete, the covariance of the results remains low, which corroborates the results obtained.

3.2 Lap shear tests

The results obtained for the five coupons for both grinder and grit sandpaper surface treatments are presented in Figures 16 and 17, respectively (the displacements have been measured with the crosshead of the testing machine and represent the vertical component of the movement of the composite laminate). In general, for both cases, a linear evolution is observed until reaching the maximum load, which is where the test finishes. In some coupons, previous failures can be observed (as the load briefly descends and then continues increasing), related presumably to preliminary debondings associated with zones where the composite and concrete were not properly joined. The mean of the values obtained for each set of coupons, the standard deviation and the covariance are shown in Table 2. It can be seen that for the case of the grinder-treated coupons, the peak loads obtained are higher, and the dispersion of the values is smaller than for the case of the grit sandpaper-treated coupons. Notice the difference in the evolution of the curves between the lap peeling and the lap shear tests. After a linear evolution in both cases, a smooth descent is found in the lap peeling tests due to the progressive nature of its failure, while in the case of the lap shear tests, a fast descent appears related to its explosive failure.

The explanation of these differences can be found by observing the fracture surfaces of both configurations (Figures 18(a) and 18(b)). In the case of the grinder-treated coupons, the adhesion is of a higher level, making the crack propagate throughout the concrete, and even involving the cracking of stones. In the case of the grit sandpaper-treated coupons, the failure is superficial, giving smaller values for the strength of the joint. The small dispersion of the values in the grinder-treated coupons is related to the fact that in this case, the shear failure force is directly related to the strength of the concrete and is less than the mechanical properties of the joint.

Although the purpose of the paper is the comparison of experimental values as a function of different features associated to the performance of the joint, a comparison with some predictions taken from the literature is going to be presented. In particular, the models by Maeda et al. [22], van Gemert [23] and Chen and Teng [24] are going to be considered. Table 3 includes the predictions with the three aforementioned models as well as the experimental values obtained, in terms of the average values of the failure load of the joint, for the grinder and the grit sandpaper surface treatments. Notice that the models do not have any parameter covering the way of preparation of the interface. It can be seen that the models by Maeda et al. and Chen and Teng lead to reasonable prediction of the failure load. On the contrary, the model by van Gemert leads to under prediction of the failure load, a fact already mentioned by Chen and Teng [24] with reference to the applicability of this model.

3.3 Pull off tests

The results of the mean maximum pull off load are shown in Table 4 with the respective statistical values for all the configurations tested (the superscript of the covariances show the zones of the block where the coupons have been extracted). In all cases, the failure of the coupons occurs inside the concrete, validating the joint. The failures of the coupons manufactured by infusion and with the grinder surface treatment (those having one of the best performances) are shown in Figure 19. The failure of the concrete can be observed at different depths: in some coupons, the failure occurs at the trepan depth (15 mm) and in others at smaller depths. Both the cement and aggregates appear broken on the fracture surface. Despite of failing in all cases inside the concrete, in the case of the grinder-treated coupons, the dispersion of the results is noticeable and, in the grit sandpaper-treated coupons, the dispersion is reasonably low. Another surprising result is that the manufacturing method of the composite apparently affects the maximum load that the joint reaches, but the failure occurs in the concrete. The explanation for these facts can be obtained from the zone of the concrete block that the coupons were obtained from. As mentioned before, the coupons were extracted from different faces of the concrete (Figure 20). Three zones have been differentiated (note that, as mentioned before, the upper face of the blocks was not used), one at the lower face of the block (zone 1) and two at the lateral face (zones 2 and 3). The coupon sets with the highest mechanical properties and lowest dispersion were obtained from zone 1. The others were extracted from zones 2 and 3, with coupons obtained from zone 2 achieving higher mechanical properties.

The reason for this behaviour is that the concrete at zone 1 is better compacted and more homogeneous. At the lateral face, the lower areas are more compacted than the upper ones, offering better properties.

3.4 Shear torsion tests

The results of the mean maximum shear torsion load are shown in Table 5, with the respective statistical values (and the zones of the block where the coupons have been extracted), for all the configurations tested. It can be appreciated that the values obtained are reasonably close, as the failure of the coupons occurred inside the concrete (just as in the case of the pull off tests), thus validating the concrete-composite joint in all cases. Again, the different areas where the coupons were extracted conditioned the results. The lowest strength values and higher dispersion have been obtained from the coupons located closer to the upper surface of the concrete block.

The failure of the coupons manufactured by infusion and with the grinder surface treatment is shown in Figure 21. The failure of the concrete described a helix-like fracture surface (as expected because of the shear stress distribution derived from the load applied), implying the break of both cement and aggregates.

4. Conclusions and future work

The objective of this work is the evaluation of the quality of the joint between carbon fibre/epoxy composite material and concrete under: different surface treatments of the concrete and several manufacturing procedures of the composite. To this end, four types of tests, two surface treatments and three manufacturing procedures have been performed.

Globally, the following conclusions concerning the variables of the study can be found:

1) Surface treatment: it has been found that the most aggressive treatment, i.e., the grinder, least to the best mechanical properties of the joint. This fact has been clearly appreciated when performing the Lap peeling and the Lap shear tests, as in the other tests, no effect was appreciated, because the failure occurred inside the concrete. This effect is related with the depth that each treatment achieves, in the case of the grinder eliminating the superficial face of the concrete and attacking even the aggregates, and, in the case of the grit sandpaper, only affecting the surface. The irregular and deep surface generated by the grinder allows a large and strong bonding surface to be created, improving the mechanical adhesion of the composite to the concrete.

2) Manufacturing technique: the results of the Pull off and the Shear torsion tests, where the three manufacturing procedures were used, showed no differences among them, due to the appearance of the failure inside the concrete in these two tests.

To precure the laminates has some limitations, as the procedure does not allow the irregularities of the surface of the concrete to be adapted, some zones remaining not bonded. This has been observed in the Lap peeling and Lap shear tests. Consequently, this procedure cannot be recommended as it leads to a descent in the properties at failure.

Comparing the infusion and the wet hand lay-up processes, the first one is recommended, as it reduces the human factor (as the distribution of the resin is automated) and allows better properties for the composite material to be obtained (it gives a high compaction level and in that way, better fibre areal weight).

3) Tests: Due to different levels of compaction during the curing of the concrete, the different faces of the concrete blocks present different properties. This is a crucial factor to be considered when performing these types of tests, because the dispersion obtained can render the results useless.

In general terms, a further development would be to adapt the lap peeling test to a universal testing machine in order to obtain the load-displacement evolution along the entire test.

Finally, at the present stage of the technology, note that the two first tests shown (i.e., lap shear and lap peeling) can only be performed in a laboratory setting, whereas the two others (i.e., pull off and shear torsion) can be performed at an in situ level (i.e., directly on a building under construction). In this way, if possible, it would be interesting to correlate the results obtained in both sets of tests to obtain more information about their representativeness when the latter set is in situ performed.

Acknowledgements

This research was conducted with the support of the Spanish Ministry of Economy and Competitiveness in the framework of Feder-Innterconecta (Project ITC-20131020). The authors want to thank the collaboration of the companies CEMOSA and VORSEVI, who were also involved in the project.

References

1. Motavalli M, Czaderski C. FRP Composites for Retrofitting of Existing Civil Structures in Europe: State-of-the-Art Review. In: International conference of composites & polycon 2007. Tampa, October, 2007.

2. Yan F, Lin Z, Zhang D, Gao Z, Li M. Experimental study on bond durability of glass fiber reinforced polymer bars in concrete exposed to harsh environmental agents: Freeze-thaw cycles and alkaline-saline solution. Compos Part B Eng 2017; 116: 406-421.

3. Fib bulletin 14, FIB TG 9.3 FRPEBR. Externally bonded FRP reinforcement for RC structures. Fédération Internacionale du béton (Fib), Task Group 9.3 FRP, 2001.

4. CNR DT200 Guide for the design and construction of an externally bonded FRP system for strengthening existing structures. Italian National Research Council, Rome, 2013.

5. Garbacz A, Górka M, Courard L. Effect of concrete surface treatment on adhesion in repair systems. Mag Concr Res 2005; 57(1): 49-60.

6. Garbacz A, Courard L, Bissonnette B. A surface engineering approach applicable to concrete repair engineering. Bull Polish Acad Sci: Tech Sci 2013; 61(1): 73–84.

7. Courard L, Piotrowski T, Garbacz A. Near-to-surface properties affecting bond strength in concrete repair. Cem Concr Compos 2013; 46: 73-80.

8. Garbacz A, Courard L, Kostana K. Characterization of concrete surface roughness and its relation to adhesion in repair systems. Mater Charact 2006; 56(4-5): 281-289.

9. Butler M, Mechtecherine V, Hemplel S. Durability of textile reinforced concrete made with AR glass fibre: effect of matrix composition. Mater Struct 2010; 43(10): 1351-1368.

10. Czaderski C, Martinelli E, Michels J, et al. Effect of curing conditions on strength development in an epoxy resin for structural strengthening. Compos Part B Eng. 2012; 43(2):398–410.

11. Courard L. Parametric Study for the Creation of the Interface between Concrete and Repair Products. Mater Struct 2000; 33(1): 65-72.

12. Carozzi FG, Bellini A, D'Antino T, de Felice G, Focacci G, Hojdys L, et al. Experimental investigation of tensile and bond properties of Carbon-FRCM composites for strengthening masonry elements. Compos Part B Eng 2017; 128: 100-119.

13. D'Antino T, Pisani MA, Poggi C. Effect of the environment on the performance of GFRP reinforcing bars. Compos Part B Eng 2018; 141: 123-136.

14. Karbhari VM, Engineer M, Eckel DA. On the durability of composite rehabilitation schemes for concrete: use of a peel test. J Mater Sci 1997; 32(1): 147-156.

15. Mata OR, Atadero RA. Evaluation of Pull-Off Tests as a FRP– Concrete Bond Testing Method in the Laboratory and Field. Practice Periodical on Structural Design and Construction 2014; 19(2).

16. Wang Z, Khalid HR, Seo JH, Kang J, Lee HK. Pull-off bond behavior of anchored random-chopped FRP composites bonded to concrete. Compos Struct 2018; 185: 193-202.

17. ASTM D4541-17, Standard Test Method for Pull-Off Strength of Coatings Using Portable Adhesion Testers. ASTM International, West Conshohocken, PA, 2017.

18. Ţăranu N, Oltean R, Cozmanciuc C-I. Experimental investigation on bonding carbon fiber reinforced polymeric plates to concrete substrate. Bul Inst Polit Iaşi t 2011; LVII (LXI), f. 3.

19. Hosseini A, Mostofinejad D. Effective bond length of FRP-to-concrete adhesively-bonded joints: Experimental evaluation of existing models. Int J Adhes Adhes 2014; 48: 150-158.

20. Oltean R, Cozmanciuc C, Munteanu V. Adhesive Bonding Techniques in Hybrid Structured Made from Fibre Reinforced Composites and Concrete. Bul Inst Polit Iaşi s Constr Archit 2009; LV (LIX), 3: 67-72.

21. Williams C, Summerscales J, Grove S. Resin Infusion Under Flexible Tooling. Compos Part A Appl Sci Manuf 1996; 27(7): 517-524.

22. Maeda T, Asano Y, Sato Y, Ueda T, and Kakuta Y. A study on bond mechanism of carbon fiber sheet. Non-Metallic (FRP) Reinforcement for Concrete Struct., Proc., 3rd Int. Symp., Japan Concrete Institute 1997; 1: 279–285.

23. van Gemert D. Force transfer in epoxy-bonded steel-concrete joints. Int. J. Adhesion and Adhesives 1980; 1: 67–72.

24. Chen J-F, Teng JG. Anchorage strength models for FRP and steel plates bonded to concrete. J Struct Eng 2001;127(7): 784-791.

Figures

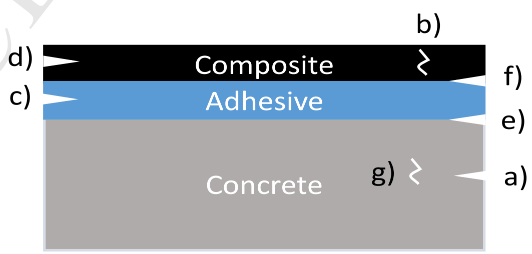

Figure 1. Possible failure modes of the composite-concrete joint

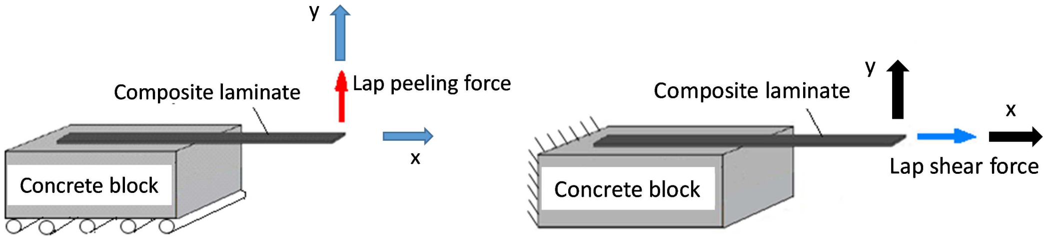

(a) (b)

Figure 2. (a) Scheme of the lap peeling test. (b) Scheme of the lap shear test

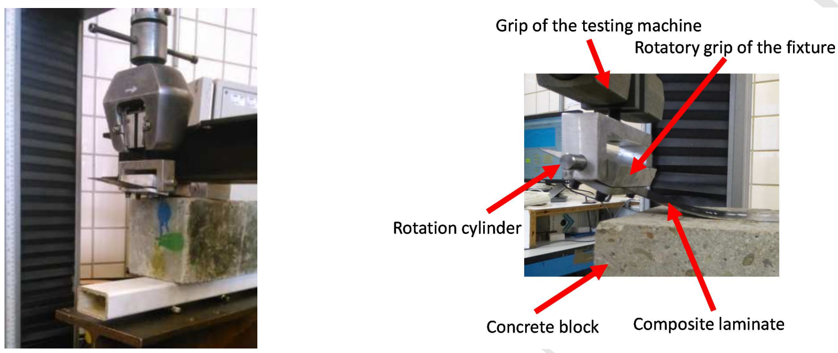

(a) (b)

Figure 3. (a) Lap peeling test fixture. (b) Detail of the fixing tool for the lap peeling test

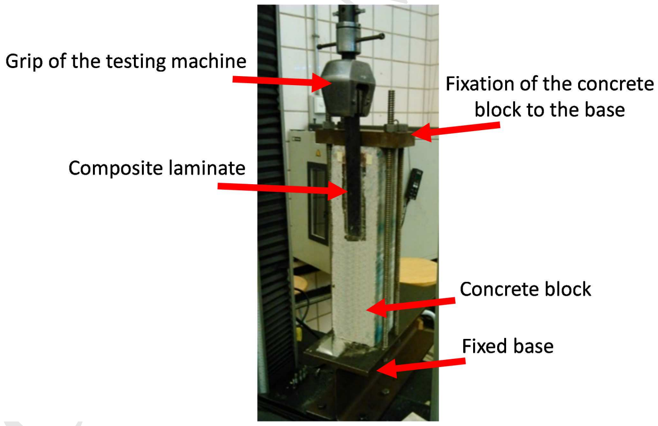

Figure 4. Lap shear test fixture

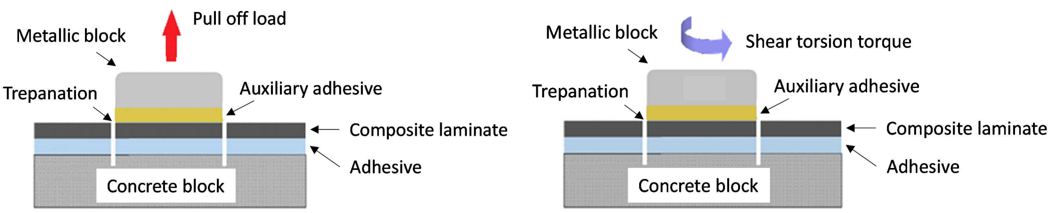

(a) (b)

Figure 5. (a) Scheme of the pull off test. (b) Scheme of the shear torsion test

(a) **(b)**

Figure 6. (a) View of the pull off testing machine. (b) Detailed view of the connection of the pull off machine to the coupon

Figure 7. Shear torsion test fixture

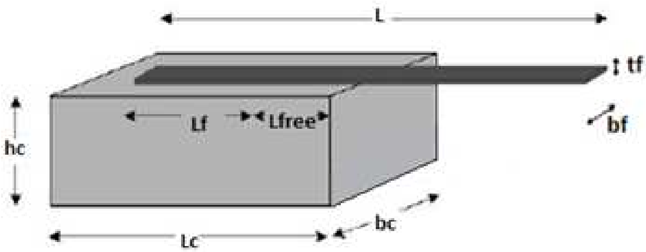

CONCRETE	COMPOSITE
h_c = 150 mm	t_f = 2 mm
b_c = 150 mm	b_f = 45 mm
L_c = 600 mm	L_f = 200 mm
	L_{free} = 50 mm
	L = 400 mm

Figure 8. Geometry and dimensions of the lap peeling and lap shear coupons

(a) **(b)**

Figure 9. (a) Protection of the concrete block after the bonding. (b) Composite laminate bonded to the concrete block in a lap peeling/ lap shear coupon

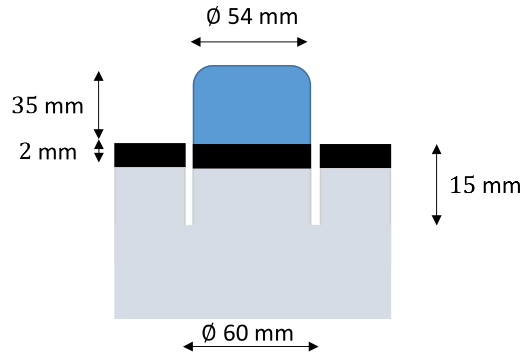

Figure 10. Geometry and dimensions of the pull off and shear torsion coupons

(a)

(b)

Figure 11. (a) Trepanation of the composite-concrete joint. (b) Bonding of the metallic blocks for the pull off/shear torsion coupons

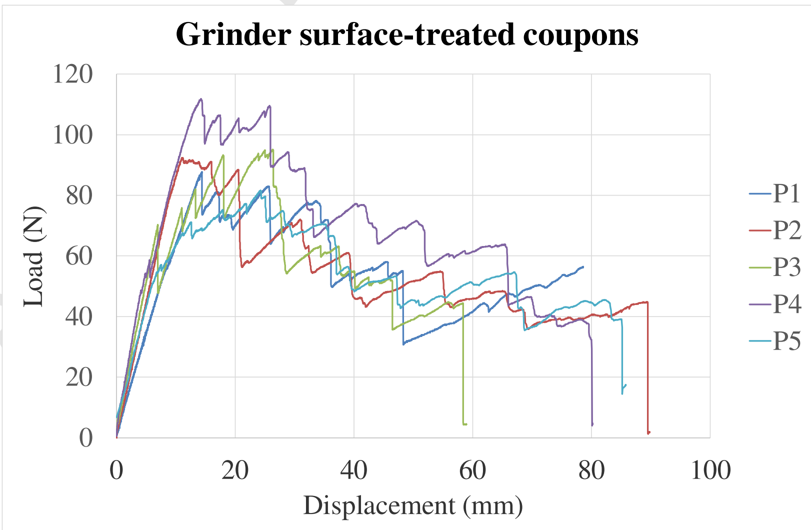

Figure 12. Load/displacement curve of the lap peeling test for the grinder surface-treated coupons

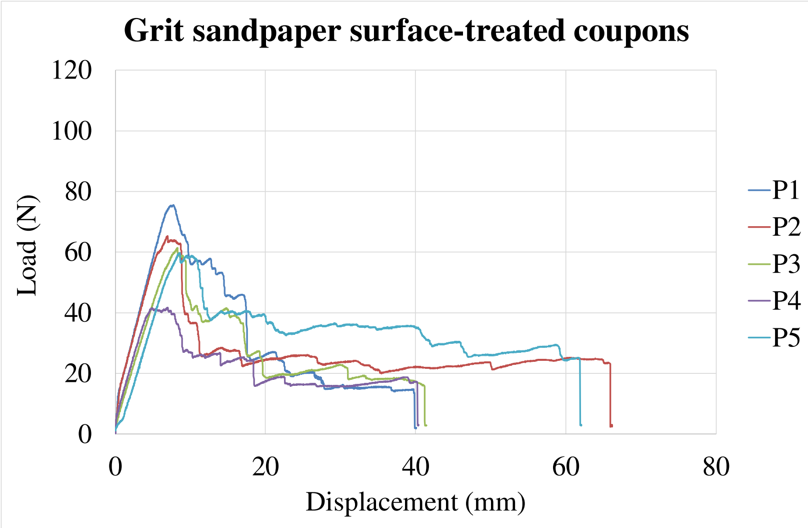

Figure 13. Load/displacement curve of the lap peeling test for the grit sandpaper surface-treated coupons

(a) **(b)**

Figure 14. Composite failure surfaces after the lap peeling test for (a) grinder surface-treated coupons and (b) grit sandpaper surface-treated coupons

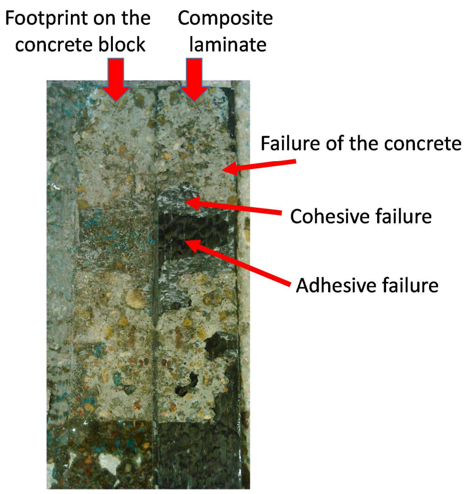

Figure 15. Detail of the failure surfaces of the concrete and the composite of a grinder surface-treated coupon after the lap peeling test. The coupon corresponds to the first coupon of Figure 11(a)

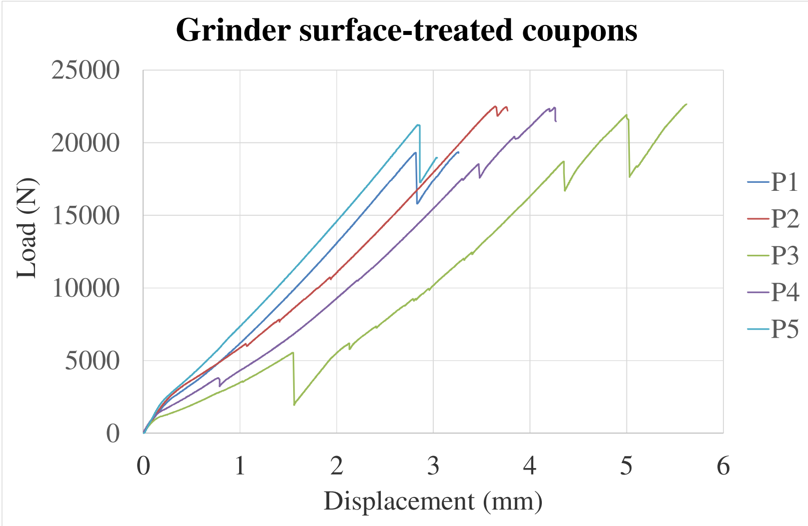

Figure 16. Load/displacement curve of the lap shear test for the grinder surface-treated coupons

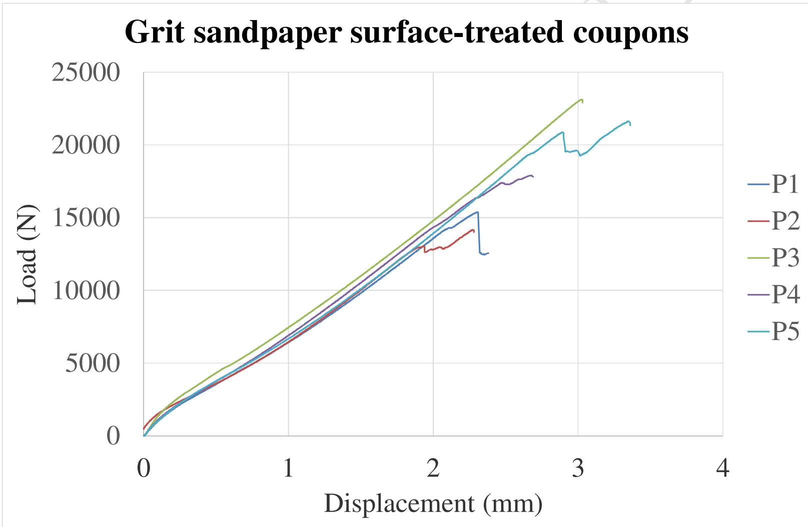

Figure 17. Load/displacement curve of the lap shear test for the grit sandpaper surface-treated coupons

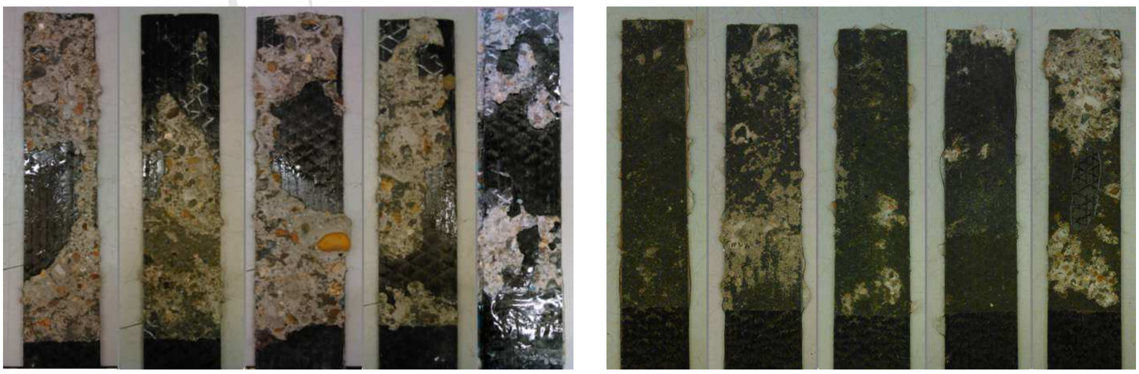

(a) (b)

Figure 18. Composite failure surfaces after the lap shear test for (a) grinder surface-treated coupons and (b) grit sandpaper surface-treated coupons

Figure 19. Failure of the grinder surface-treated, infusion manufactured pull off coupons

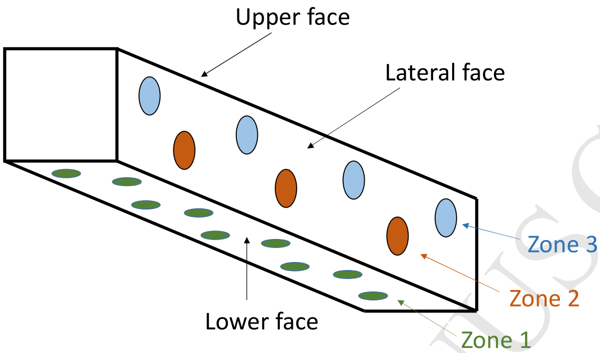

Figure 20. Scheme of the concrete block zones where the pull off coupons were extracted

Figure 21. Failure of the grinder surface-treated, infusion manufactured shear torsion coupons

Surface treatment	Mean max. load (N)	Standard deviation (N)	Covariance (%)
Grinder	93.71 (154.38%)	11.34	12.10
Grit sandpaper	60.70 (100%)	12.29	20.25

Table 1. Mean, standard deviation and covariance of the results of the lap peeling test for the grinder and grit sandpaper coupons

Surface treatment	Mean max. load (N)	Standard deviation (N)	Covariance (%)
Grinder	21631.05 (117.36%)	1392.90	6.44
Grit sandpaper	18431.03 (100%)	3873.46	21.02

Table 2. Mean, standard deviation and covariance of the results of the lap shear test for the grinder and grit sandpaper coupons

	Experimental values		Theoretical predictions		
	Grinder	Grit sandpaper	Maeda et al.	van Gemert	Chen and Teng
Failure load (kN)	21.63	18.43	20.40	14.97	22.50

Table 3 Experimental failure load of the joints versus predictions of several theoretical models.

	Manufacturing procedure								
	Pre-cured			Hand lay-up			Infusion		
Surface treatment	Mean max. load (N)	Standard deviation (N)	Covariance (%)	Mean max. load (N)	Standard deviation (N)	Covariance (%)	Mean max. load (N)	Standard deviation (N)	Covariance (%)
Grinder	4969 (120.46%)	1830.08	36.83[2,3]	4125 (100%)	1806.34	43.79[3]	7148 (173.28%)	1212.30	16.96[2]
Grit sandpaper	5121 (124.14%)	853.67	16.67[1]	7621 (184.75%)	933.57	12.25[1]	6630 (160.73%)	1190.75	17.96[1]

Table 4. Mean, standard deviation and covariance of the results of the pull off test for the grinder and grit sandpaper coupons for all the manufacturing methods

	Manufacturing procedure								
	Pre-cured			Hand lay-up			Infusion		
Surface treatment	Mean torque (Nm)	Standard deviation (Nm)	Covariance (%)	Mean torque (Nm)	Standard deviation (Nm)	Covariance (%)	Mean torque (Nm)	Standard deviation (Nm)	Covariance (%)
Grinder	107 (105.94%)	7.90	7.38[2]	119 (117.82%)	10.50	8.82[1]	111 (109.90%)	15.90	14.32[2]
Grit sandpaper	133 (131.68%)	11.23	8.44[1]	101 (100%)	15.39	15.24[2]	136 (134.65%)	32.10	23.60[1]

Table 5. Mean, standard deviation and covariance of the results of the shear torsion test for the grinder and grit sandpaper coupons for all the manufacturing methods